Dear Med Chem Students and Faculty,

I plan to compare two papers for this Monday Night Meeting - both seem short so hopefully you have time to read or skim them. Both are attached in this PDF.

Thanks,

Michelle

Paper One:

Active site proton delivery and the lyase activity of human CYP17A1
Yogan Khatri, Michael C. Gregory, Yelena V. Grinkova, Ilia G. Denisov, Stephen G. Sligar

Paper Two:

Mechanism of the Third Oxidative Step in the Conversion of Androgens to Estrogens by Cytochrome P450 19A1 Steroid Aromatase
Francis K. Yoshimoto and F. Peter Guengerich

Biochemical and Biophysical Research Communications 443 (2014) 179–184

Contents lists available at ScienceDirect

Biochemical and Biophysical Research Communications

journal homepage: www.elsevier.com/locate/ybbrc

Active site proton delivery and the lyase activity of human CYP17A1

Yogan Khatri, Michael C. Gregory, Yelena V. Grinkova, Ilia G. Denisov, Stephen G. Sligar *

Department of Biochemistry, University of Illinois at Urbana Champaign, 116 Morrill Hall, 505 S. Goodwin Avenue, Urbana, IL 61801, United States

ARTICLE INFO

Article history:
Received 7 November 2013
Available online 2 December 2013

Keywords:
CYP17A1
T306A
Proton delivery
Compound I
Nucelophilic attack

ABSTRACT

Cytochrome P450 CYP17A1 catalyzes a series of reactions that lie at the intersection of corticoid and androgen biosynthesis and thus occupies an essential role in steroid hormone metabolism. This multifunctional enzyme catalyzes the 17α-hydroxylation of Δ4- and Δ5-steroids progesterone and pregnenolone to form the corresponding 17α-hydroxy products through its hydroxylase activity, and a subsequent 17,20-carbon–carbon scission of pregnene-side chain produce the androgens androstenedione (AD) and dehydroepiandrosterone (DHEA). While the former hydroxylation reaction is believed to proceed through a conventional "Compound I" rebound mechanism, it has been suggested that the latter carbon cleavage is initiated by an iron-peroxy intermediate. We report on the role of Thr306 in CYP17 catalysis. Thr306 is a member of the conserved acid/alcohol pair thought to be essential for the efficient delivery of protons required for hydroperoxoanion heterolysis and formation of Compound I in the cytochromes P450. Wild type and T306A CYP17A1 self-assembled in Nanodiscs were used to quantitate turnover and coupling efficiencies of CYP17's physiological Δ4- and Δ5-substrates. We observed that T306A co-incorporated in Nanodiscs with its redox partner cytochrome P450 oxidoreductase, coupled NADPH only by 0.9% and 0.7% compared to the wild type (97% and 22%) during the conversion of pregnenolone and progesterone, respectively, to the corresponding 17-OH products. Despite increased oxidation of pyridine nucleotide, hydroxylase activity was drastically diminished in the T306A mutant, suggesting a high degree of uncoupling in which reducing equivalents and protons are funneled into non-productive pathways. This is similar to previous work with other P450 catalyzed hydroxylation. However, catalysis of carbon–carbon bond scission by the T306A mutant was largely unimpeded by disruption of the CYP17A1 acid-alcohol pair. The unique response of CYP17A1 lyase activity to mutation of Thr306 is consistent with a reactive intermediate formed independently of proton delivery in the active site, and supports involvement of a nucleophilic peroxo-anion rather than the traditional Compound I in catalysis.

1. Introduction

The human microsomal cytochrome P450, CYP17A1, is a key enzyme in steroid hormone biosynthesis, which is capable of both hydroxylase and carbon–carbon lyase activity in a series of chemical transfomations of pregnenolone that give rise to corticoid precursors and androgens. In human adrenal steroidogenesis, the hydroxylation process predominates in the *adrenal zona fasciculata*, where Δ5 (pregnenolone, PREG) and Δ4 (progesterone, PROG) steroid are converted into the 17α-hydroxy products OH-PREG and OH-PROG, respectively, by insertion of an oxygen into a C–H bond. In the *adrenal zona reticularis*, each of these hydroxylated products are converted to the estrogen and testosterone precursors dehydroepiandrosterone (DHEA) and androstenedione (AD) via 17,20-carbon–carbon bond scission in which the 21-carbon 17α-hydroxysteroids are cleaved to 19-carbon, 17-ketosteroids, and acetic acid [1]. This compartmentalization of CYP17A1 behavior in the adrenal gland is thought to be controlled by co-localization with its putative allosteric effector cytochrome b_5 (cyt-b_5) in the *adrenal zona reticularis* [2–4]. Interaction between CYP17A1 and cyt-b_5 is known to substantially stimulate C–C lyase activity of this enzyme such that its presence can be considered essential for lyase chemistry. Furthermore, the absence of CYP17A1 in the *adrenal zona glomerulosa* helps to direct steroidogenesis in this region toward mineralocorticoid aldosterone production. As a result, varying expression levels of CYP17A1 and cyt-b_5 throughout the adrenal gland controls an important branch point in human steroidogenesis between glucocorticoid and sex hormone biosynthesis. It has been shown that both PREG and PROG are good substrates for human CYP17A1 for the 17α-hydroxylase reaction, however, 17-OH-PREG is preferred over 17-OH-PROG for the 17,20-lyase reaction [5–7].

The C–C lyase reaction catalyzed by CYP17A1 is notable not only for the profound rate enhancement exerted by association

Abbreviations: PREG, pregnenolone; OH-PREG, 17α-hydroxy-pregnenolone; PROG, progesterone; OH-PROG, 17α-hydroxy-progesterone; DHEA, dehydroepiandrosterone; AD, androstenedione; cyt-b_5, cytochrome b_5; Cpd I, Compound I.

* Corresponding author. Fax: +1 (217) 265 4073.
E-mail address: s-sligar@illinois.edu (S.G. Sligar).

0006-291X/$ - see front matter © 2013 Elsevier Inc. All rights reserved.
http://dx.doi.org/10.1016/j.bbrc.2013.11.094

with cyt-b_5, but also in the chemistry performed. While the hydroxylase activity of CYP17A1 is expected to proceed through the "Compound I" initiated hydrogen abstraction observed in other members of the P450 superfamily, significant debate exists regarding the nature of the intermediate responsible for catalysis of carbon–carbon bond scission. The nucleophilic peroxoanion attacking the C-20 carbonyl of OH-PREG and OH-PROG with subsequent decomposition to form the androgen product was suggested [8–10]. On the other hand, the traditional mechanism catalyzed by Compound I (Cpd I) has also been proposed [11].

Decades of interrogation of the cytochromes P450, including the mechanistic exemplar for this family of enzymes, P450cam, has yielded a wealth of information regarding the key catalytic intermediates and active site environment necessary for the generation of the Cpd I high-valent porphyrin cation radical utilized in hydrogen abstraction and substrate hydroxylation, thought to operate in all P450s (Fig. 1) [12–14]. Of a particular relevance to this study is the structural motif of the I-helix and its conserved residue Threonine (Thr), located in the distal side of the heme-plane [15]. Thr252 in P450cam plays an important role in proton transfer essential for O–O bond scission required for Cpd I formation [16–18], and dioxygen activation during catalytic turnover [19,20]. It has been shown that mutation of this Thr residue to Ala results in a dramatic inhibition of substrate hydroxylation catalyzed by several P450s such as CYP102A1 (P450BM3) [21], CYP2E1 [22,23], CYP2D6 [24] and CYP1A2 [25]. The critical role of this threonine in successful formation of Cpd I and productive catalysis in cytochromes P450 is now well established [18,26,27].

In this work, we evaluate the mechanistic differences in the two steps reaction comprised with hydroxylation and lyase activity performed by CYP17A1 using the analogous mutation, T306A, within steroid metabolizing P450. Previously, Akthar's group studied the T306A mutant of CYP17A1, using Δ5-steroids (PREG and 17-OH-PREG) as substrates [9]. Other reports of CYP17A1 activity used various subsets of Δ4- and Δ-5-steroids as substrates and detergent solubilized CYP17A1 reconstituted with CPR and cyt-b_5 at different stoichiometries [8,9,28–30], which makes a direct comparison of the hydroxylase and lyase activity for specific Δ4- or Δ5-steroids difficult. To overcome these shortfalls, we incorporated CYP17A1 and its variant T306A in Nanodiscs and reconstituted it with redox partners in a well controlled stoichiometry [31,32]. We also employed the consistent substrate sets, the Δ5 (PREG and 17-OH-PREG) and Δ4 (PROG and 17-OH-PROG) steroids to study the hydroxylase and lyase activity using the same preparation of cytochrome P450 reductase (CPR) and cyt-b_5 throughout the *in vitro* reconstitution experiments. Importantly, we also documented the preference of substrate and coupling efficiency during the hydroxylation and lyase reaction by the wild type CYP17A1 and its mutant T306A.

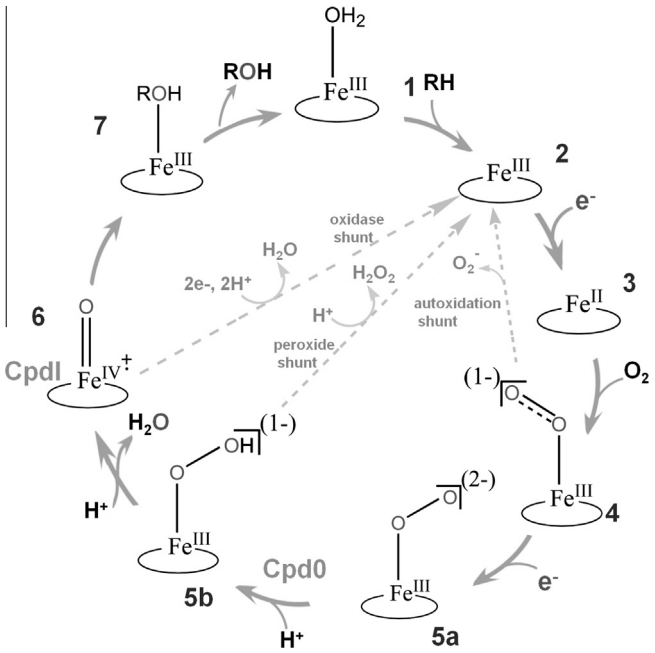

Fig. 1. A reaction cycle of cytochrome P450 catalysis. The seven steps indicating the binding of substrate (**1**), formation of a high spin ferric state (**2**), transfer of an electron from the redox partner to form the ferrous protein (**3**), generation of the ferrous oxygenated (oxy-ferrous) state (**4**), reduction to form the peroxo states after receiving second electron (**5a**), transfer of proton to the distal oxygen atom and production of the "hydroperoxo" state (**5b**), a second protonation and formation of a higher valent metal-oxo species "Compound I" (Cpd I) (**6**), and the hydroxylation and release of product (**7**) of P450 catalysis are illustrated. The three unproductive pathways are shown in grey. (For interpretation of color in this Figure, the reader is referred to the web version of this article.)

2. Materials and methods

2.1. Construction of T306A

In order to obtain the conserved I-helix variant of human CYP17A1 T306A, the pCWori_CYP17A1 construct [7] was mutated using primers 5′-ggt gcc ggt gtg gaa gcc acc acc agc gtc gtc-3′ (forward) and 5′-gac gac gct ggt ggt ggc ttc cac acc ggc acc-3′ (reverse). The sequence of the mutant was verified by automated DNA sequencing (ACGT, Inc.).

2.2. Expression and purification of recombinant proteins

The expression and purification of T306A was performed as described for wild type CYP17A1 [7,33]. The expression and purification of membrane scaffold protein (MSP), rat P450 reductase (CPR) and cyt-b_5 was performed as described [34–36].

2.3. Nanodisc assembly of T306A

The detailed protocol for the incorporation of CYP17A1 into Nanodiscs has been previously reported [7,33] and same procedure was employed for the T306A mutant.

2.4. Spectroscopic characterization

UV–visible spectra for CYP17A1 and T306A were recorded at room temperature using a Cary 300 UV–visible spectrophotometer. The P450 concentration was estimated by CO-difference spectra assuming $\Delta\varepsilon(450–490) = 91\ mM^{-1}\ cm^{-1}$ as described [37].

2.5. NADPH oxidation

Incorporation of CPR into preformed and purified CYP17A1 (or T306A) Nanodiscs was made by direct addition of oligomeric CPR at 1:4 CYP17A1 (or T306A)/CPR molar ratio, as described [38]. Briefly, 1 ml of CYP17A1 (or T306A) and CPR solution, in presence or absence of cytochrome b_5 (1:4:4 M ratio), in 100 mM potassium phosphate buffer, pH 7.4, containing 50 mM NaCl and 50 μM substrate (PROG, 17-OH-PROG, PREG or 17-OH-PREG) was brought 37 °C in a stirred quartz cuvette. The sample was incubated for 5 min and the reaction was initiated by addition of 100 μM of NADPH. The consumption of NADPH was monitored by recording the absorbance at 340 nm for 5 min. The reaction was stopped by adding 50 μl of 9 M sulfuric acid to bring the pH below 4.0. The sample was removed from the cuvette, flash frozen in liquid nitrogen, and stored at −80 °C until product analysis. The optical

measurements were performed on Hitachi U-3300 spectrophotometer supplied with temperature controller and built-in magnetic stirrer. For 17-OH-PROG and 17-OH-PREG assay a threefold higher concentration of NADPH was used with a path length of 0.4 cm rather than 1 cm. The rate of NADPH oxidation was determined from the slope of absorption at 340 nm during the first 2 min using an extinction coefficient of 6.22 cm^{-1} mM^{-1}.

2.6. Catalytic turnover

Analysis of the hydroxylated and lyase products of Δ4- and Δ5-steroids by CYP17A1 and T306A was performed as follows.

The conversion of PREG to 17-OH-PREG was analyzed by TLC (EMD TLC Silica gel 60 F254, 20 × 20 cm), using radiolabeled [7-^{3}H] pregnenolone (8.5 nmol, 0.8 μCi) as described [39]. The conversion of PROG to 17-OH-PROG was analyzed by HPLC (Waters). Briefly, 1 μl of 27 mM cortexolone solution in methanol were added to 500 μl each of the reaction sample and vortexed for 10 s. 2 ml of chloroform was added to each aliquots and vortexed for 30 s. The organic phage was removed and dried under the stream of nitrogen. The dried sample was dissolved in 100 μl of methanol and 40 μl was injected onto C_{18}-HPLC column, using a 150 × 2.1 mm, 3 μm (ACE-111-1502) with the mobile phase of 45% each of methanol and acetonitrile in water and a flow rate of 0.2 ml/min. The 17-hydroxylated product of PROG was separated in the linear gradient of methanol and acetonitrile from 20% to 80% in 28 min. Peak integration was performed with GRAM/32 software (Thermo Fischer Scientific). The analysis of 17-hydroxylated product of both Δ4- and Δ5-steroids was performed on an FID equipped gas chromatograph (Agilent 6890) as described [39].

3. Results

3.1. Expression, purification, spectrophotometric characterization and assembly of T306A Nanodiscs

The mutant protein T306A was successfully overexpressed and purified from the bacterial membrane. The protein was pure by SDS–PAGE with a mass of ~58 kDa. The yield of the protein was 4–6 mg/L *Escherichia coli* cell culture. The oxidized, reduced and CO-complexed spectra of the progesterone bound T306A displayed the Soret band at 391 nm, a diminished absorption maximum at 408 and 447 nm, respectively. The mutant protein was incorporated into Nanodiscs and the purity was confirmed by SDS–PAGE and HPLC size exclusion chromatography. The oxidized substrate free T306A showed the characteristic absorption maxima: Q bands at 568 nm (α band) and 535 nm (β band), and the Soret band at 417 nm. The pronounced Soret peak at 417 nm in the absence of substrate was shifted to 391 nm by the addition of progesterone. The reduced protein displayed a peak maximum at 408 nm and the reduced CO-complex showed a typical "P450" peak at 447 nm.

3.2. NADPH oxidation and turnover of Δ4- and Δ5-steroids by CYP17WT and T306A

The rates of pyridine nucleotide oxidation and product formation were measured for T306A and compared with that of the wild type enzyme. We evaluated both the hydroxylase and lyase activities in the presence of Δ4- and Δ5-steroids. Using PREG and PROG as substrates, the "normal" hydroxylation reaction is followed by the production of the 17α-OH product. Using 17-OH-PREG and 17-OH-PROG allowed us to specifically examine the 17,20-carbon–carbon lyase reaction of the corresponding substrates by monitoring the production of dehydroepiandrosterone (DHEA) and androstenedione (AD), respectively. Since Thr306 is a member of the conserved acid/alcohol pair and thought to be essential for the efficient delivery of protons required for hydroperoxoanion heterolysis and formation of Cpd I in P450cam [16,28,18], the change of T306A at the analogous position in CYP17A1 would be expected to disrupt the Cpd I mediated hydroxylation chemistry. We observed that T306A consumed NADPH at about 6.6 and 2.3 times faster than WT during the conversion of PREG and PROG, respectively, to their corresponding 17α-OH product (Fig. 2A, Table 1). However, the product formation rate was dramatically reduced by ~94% and 92% (Fig. 2B, Table 1). As a result, the coupling efficiency of T306A was less than 1% during the hydroxylation of PREG and PROG as compared to 97% and 22%, for WT (Fig. 2C). These two reactions were highly uncoupled in T306A mutant where reducing equivalents and protons are funneled into the formation of superoxide and hydrogen peroxide without O–O bond cleavage rather than productive hydroxylation of the substrates. This suggests the disruption on proton delivery to the distal oxygen atom of the peroxoanion which is required to initiate O–O bond scission and formation of the Cpd I reactive intermediate. These results are consistent with previous investigations of P450cam [16,40] and other systems, in which mutation of this critical residue severely impairs formation of Cpd I with a concomitant decoupling of product formation from NADPH oxidation.

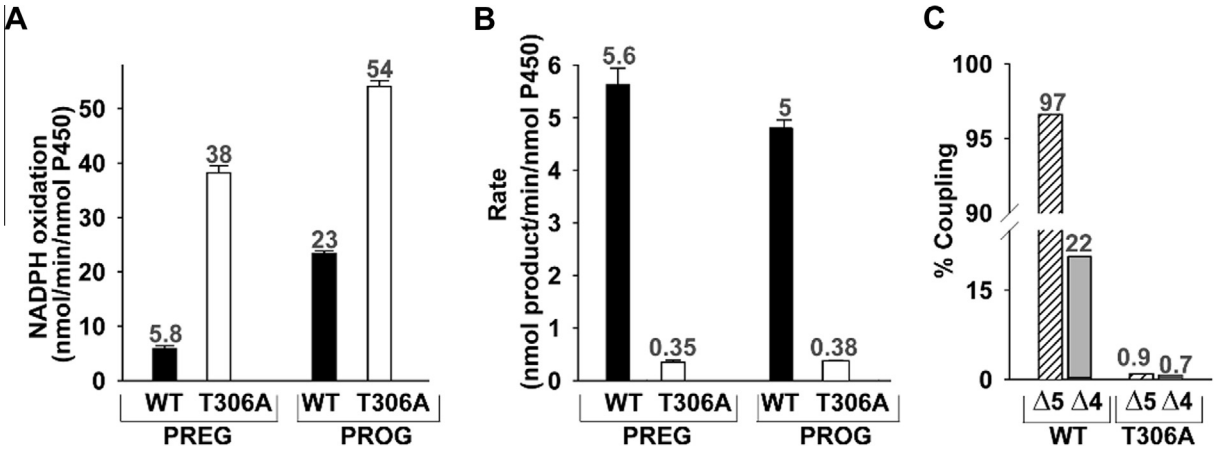

Fig. 2. Comparative study on 17-α-hydroxylase activity of pregnenolone and progesterone by wild type CYP17A1 and T306A. Determination of rate of NADPH oxidation (A) and the rate of conversion of pregnenolone (Δ5-steroid) and progesterone (Δ4-steroid) to the corresponding 17-OH-product (B) are shown. The black and open bars represent the WT and T306A, respectively. The coupling efficiency (C) of WT and T306A during the hydroxylation of Δ5-(stripped-bar) and Δ4-steroids (grey bar) are illustrated. The number on the bar represents the values of the activity. (For interpretation of color in this Figure, the reader is referred to the web version of this article.)

Table 1
Comparison of hydroxylation and lyase reactivities of Δ5- and Δ4-steroids by human CYP17A1.

Δ5-Steroid			Δ4-Steroid			Refs.
PREG → 17α-OH-PREG CYP17	17α-OH-PREG → DHEA CYP17		PROG → 17α-OH-PROG CYP17	17α-OH-PROG → AD CYP17		
$-b_5$	$-b_5$	$+b_5$	$-b_5$	$-b_5$	$+b_5$	
5.63 ± 0.31[a]	0.15 ± 0.02[b]	0.76 ± 0.21[b]	4.81 ± 0.15[c]	0.05 ± 0.01[b]	0.34 ± 0.04[b]	This study
–	0.17 ± 0.042[d]	–	2.9 ± 0.39[d]	–	–	[28]
2.20[d]	0.00[d]	2.45[d]	3.33[d]	0.00[d]	1.80[d]	[8]
2.17 ± 0.04[d]	0.32 ± 0.05[d]	3.06 ± 0.05[d]	–	–	–	[9]
–	–	–	3.5[d,e]	0.12[d,e]	0.64[d,e]	[29]
–	0.12 ± 0.001[f,c]	0.28 ± 0.03[f,c]	6.89 ± 0.24[f,c]	–	–	[30]
–	0.04 ± 0.009[c,g]	0.21 ± 0.04[c,g]	2.10 ± 0.17[c,g]	–	–	[30]

Note: Conversion monitored by [a]TLC using [7–^{3}H]PREG, [b]GC, [c]HPLC, [d]TLC using ^{3}H-labeled substrates ([^{3}H]PREG, [^{3}H]PROG, [^{3}H]17α-OH-PROG, [^{3}H]17α-OH-PREG); [e]partically purified protein; [f]full length CYP17; [g]CYP17 variant with the deletion of N-terminal hydrophobic amino acid sequence; –not studied.

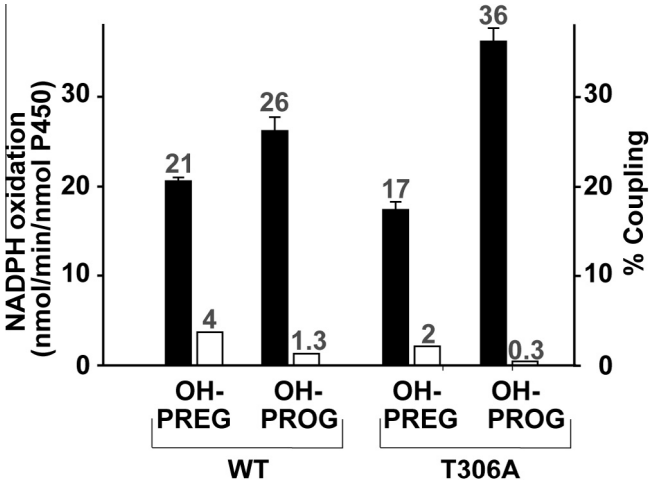

Fig. 3. Comparison of NADPH oxidation and coupling efficiency during 17,20-lyase activity by wild type CYP17A1 and T306A. Determination of rate of NADPH oxidation (black bar) and percentage of coupling (white bar) for 17-OH-PREG and 17-OH-PROG for wild type CYPC17A1 and T306A are shown. The number on the bar represents the corresponding value related with the unit on the *y*-axis. The error bar represents the standard deviation of 6–8 independent measurements.

On the other hand, catalysis of carbon–carbon bond scission by the T306A mutant was largely unimpeded by disruption of the CYP17A1 acid–alcohol pair (Fig. 3, Table 1). During carbon–carbon bond scission reaction monitored by the conversion of 17-OH-PREG to DHEA, the rate of NADPH oxidation was almost similar 21 vs 17 nmol/min/nmolP450 for WT and T306A, respectively, and did not show the dramatic difference in coupling (4% vs 2% for WT and mutant) (Fig. 3, Table 1). Likewise, the lyase reaction of 17α-OH-PROG to AD also showed the similar rates, having moderately increasing rate of NADPH consumption in T306A mutant, of NADPH oxidation of 26 vs 36 nmol/min/nmolP450 with the coupling of 1.3% vs 0.3% for WT and T306A. However, in both the lyase reactions, we did not observe dramatic changes like the one that we have observed during hydroxylase activity. These data suggested that C–C lyase chemistry conducted by CYP17A1 proceeds independently of the proton delivery pathway and O–O bond scission and Cpd I formation and are consistent with a reactive peroxo anion that initiates the 17,20-lyase activity through nucleophilic attack on the 20-keto group of the substrate [39].

3.3. Effect of cytochrome b_5 on the lyase reaction

It is well documented that cyt-b_5 augments the 17,20-carbon–carbon bond scission of mammalian CYP17 [2,3,41–43], although detailed studies as a function of the P450:CPR:cyt-b_5 ratio have not been reported. Therefore, we explored the effect of cyt-b_5 during lyase activity on our well defined assay system consisting of CYP17A1 Nanodiscs and co-incorporated CPR and cyt-b_5. We unambiguously observed the preference of 17-OH-PREG (>2-fold higher compared to 17-OH-PROG) during 17,20-lyase activity for both the WT and T306A (Fig. 4, Table 1) in presence of cyt-b_5. It

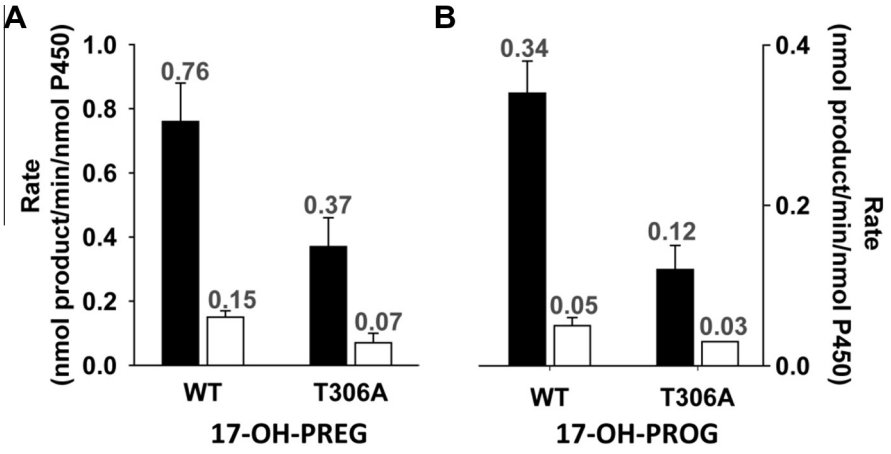

Fig. 4. Cytochrome b_5 effect on CYP17A1 lyase activity. The rate conversion of 17-OH-PREG to DHEA and 17-OH-PROG to AD was measured in the presence (black bar) and absence (white bar) of cytochrome b_5. The number on the bar represents the rate of conversion of the substrate and the error bar the standard deviation of 6–8 independent measurements.

has also been shown that the human, bovine, ovine and caprine CYP17 enzymes use 17OH-PREG as a preferred substrate for the 17,20-lyase reaction [3,41,42,44–46]. In this study, we also observed that the presence of cyt-b_5 enhanced the lyase activity by ~5- and 7-fold in the WT and ~5- and 4-fold in T306A for 17-OH-PREG and 17-OH-PROG, respectively. Though a detailed mechanism for cyt-b_5 participation in catalysis is not clear, the most recent study on NMR chemical shift mapping of cyt-b_5 titrations with CYP17A1 by Scott's group [47] showed evidence that cyt-b_5 and CPR compete for a binding surface on CYP17A1, and the CYP17A1/cyt-b_5 interaction is stronger in the presence of hydroxylase substrate pregnenolone in the CYP17A1 active site than when the presence of lyase substrate 17α-OH-progesterone.

In conclusion, we have shown that the highly conserved acid–alcohol pair in human CYP17A1 supports a proton delivery pathway necessary only for oxygen–oxygen bond scission to form Cpd I which initiates normal hydroxylation process. This residue, and the associated proton delivery, is not operating the lyase reaction. The unique response of CYP17A1 lyase activity to mutation of Thr306 is consistent with a reactive intermediate formed independently of proton delivery in the active site and suggests the involvement of a nucelophilic peroxo-anion rather than the traditional Cpd I.

Acknowledgment

This work was supported by the National Institutes of Health Grants GM31756 and GM33775.

References

[1] R.J. Auchus, W.L. Miller, Molecular modeling of human P450c17 (17α-hydroxylase/17,20-lyase): insights into reaction mechanisms and effects of mutations, Mol. Endocrinol. 13 (1999) 1169–1182.
[2] S. Kominami, N. Ogawa, R. Morimune, D.Y. Huang, S. Takemori, The role of cytochrome b5 in adrenal microsomal steroidogenesis, J. Steroid Biochem. Mol. Biol. 42 (1992) 57–64.
[3] M. Katagiri, N. Kagawa, M.R. Waterman, The role of cytochrome b5 in the biosynthesis of androgens by human P450c17, Arch. Biochem. Biophys. 317 (1995) 343–347.
[4] A.V. Pandey, W.L. Miller, Regulation of 17,20-lyase activity by cytochrome b5 and by serine phosphorylation of P450c17, J. Biol. Chem. 280 (1995) 13265–13271.
[5] G.B. Cutler, M. Glenn, M. Bush, G.D. Hodgen, C.E. Graham, D.L. Loriaux, Adrenarche: a survey of rodents, domestic animals, and primates, Endocrinology 103 (1978) 2112–2118.
[6] R.J. Auchus, The genetics, pathophysiology, and management of human deficiencies of P450c17, Endocrinol. Metab. Clin. North Am. 30 (2001) 101–119.
[7] M. Gregory, P.J. Mak, S.G. Sligar, J.R. Kincaid, Differential hydrogen bonding in human CYP17 dictates hydroxylation versus lyase chemistry, Angew. Chem. Int. Ed. Engl. 52 (2013) 5342–5345.
[8] P. Lee-Robichaud, J.N. Wright, M.E. Akhtar, M. Akhtar, Modulation of the activity of human 17α-hydroxylase-17,20-lyase (CYP17) by cytochrome b5: endocrinological and mechanistic implications, Biochem. J. 308 (1995) 901–908.
[9] P. Lee-Robichaud, M.E. Akhtar, M. Akhtar, An analysis of the role of active site protic residues of cytochrome P-450s: mechanistic and mutational studies on 17α-hydroxylase-17,20-lyase (P-45017α also CYP17), Biochem. J. 330 (1998) 967–974.
[10] M. Akhtar, J.N. Wright, P. Lee-Robichaud, A review of mechanistic studies on aromatase (CYP19) and 17α-hydroxylase-17,20-lyase (CYP17), J. Steroid Biochem. Mol. Biol. 125 (2011) 2–12.
[11] M. Akhtar, D. Corina, S. Miller, A.Z. Shyadehi, J.N. Wright, Mechanism of the acyl-carbon cleavage and related reactions catalyzed by multifunctional P-450s: studies on cytochrome P-450(17)α, Biochemistry 33 (1994) 4410–4418.
[12] T.M. Makris, R. Davydov, I.G. Denisov, B.M. Hoffman, S.G. Sligar, Mechanistic enzymology of oxygen activation by the cytochromes P450, Drug Metab. Rev. 34 (2002) 691–708.
[13] S.G. Sligar, T.M. Makris, I.G. Denisov, Thirty years of microbial P450 monooxygenase research: peroxo-heme intermediates – the central bus station in heme oxygenase catalysis, Biochem. Biophys. Res. Commun. 338 (2005) 346–354.
[14] I.G. Denisov, T.M. Makris, S.G. Sligar, I. Schlichting, Structure and chemistry of cytochrome P450, Chem. Rev. 105 (2005) 2253–2277.
[15] T.L. Poulos, B.C. Finzel, I.C. Gunsalus, G.C. Wagner, J. Kraut, The 2.6-A crystal structure of *Pseudomonas putida* cytochrome P-450, J. Biol. Chem. 260 (1985) 16122–16130.
[16] R. Raag, S.A. Martinis, S.G. Sligar, T.L. Poulos, Crystal structure of the cytochrome P-450CAM active site mutant Thr252Ala, Biochemistry 30 (1991) 11420–11429.
[17] Y. Imai, M. Nakamura, Point mutations at threonine-301 modify substrate specificity of rabbit liver microsomal cytochromes P-450 (laurate (omega-1)-hydroxylase and testosterone 16α-hydroxylase), Biochem. Biophys. Res. Commun. 158 (1989) 717–722.
[18] S. Nagano, T.L. Poulos, Crystallographic study on the dioxygen complex of wild-type and mutant cytochrome P450cam. Implications for the dioxygen activation mechanism, J. Biol. Chem. 280 (2005) 31659–31663.
[19] M. Vidakovic, S.G. Sligar, H. Li, T.L. Poulos, Understanding the role of the essential Asp251 in cytochrome p450cam using site-directed mutagenesis, crystallography, and kinetic solvent isotope effect, Biochemistry 37 (1998) 9211–9219.
[20] I. Schlichting, J. Berendzen, K. Chu, A.M. Stock, S.A. Maves, D.E. Benson, R.M. Sweet, D. Ringe, G.A. Petsko, S.G. Sligar, The catalytic pathway of cytochrome p450cam at atomic resolution, Science 287 (2000) 1615–1622.
[21] J.P. Clark, C.S. Miles, C.G. Mowat, M.D. Walkinshaw, G.A. Reid, S.N. Daff, S.K. Chapman, The role of Thr268 and Phe393 in cytochrome P450 BM3, J. Inorg. Biochem. 100 (2006) 1075–1090.
[22] K.P. Vatsis, M.J. Coon, Ipso-substitution by cytochrome P450 with conversion of p-hydroxybenzene derivatives to hydroquinone: evidence for hydroperoxo-iron as the active oxygen species, Arch. Biochem. Biophys. 397 (2002) 119–129.
[23] A.L. Blobaum, U.M. Kent, W.L. Alworth, P.F. Hollenberg, Novel reversible inactivation of cytochrome P450 2E1 T303A by tert-butyl acetylene: the role of threonine 303 in proton delivery to the active site of cytochrome P450 2E1, J. Pharmacol. Exp. Ther. 310 (2004) 281–290.
[24] P.H. Keizers, L.H. Schraven, C. de Graaf, M. Hidestrand, M. Ingelman-Sundberg, B.R. van Dijk, N.P. Vermeulen, J.N. Commandeur, Role of the conserved threonine 309 in mechanism of oxidation by cytochrome P450 2D6, Biochem. Biophys. Res. Commun. 338 (2005) 1065–1074.
[25] K. Hiroya, M. Ishigooka, T. Shimizu, M. Hatano, Role of Glu318 and Thr319 in the catalytic function of cytochrome P450d (P4501A2): effects of mutations on the methanol hydroxylation, FASEB J. 6 (1992) 749–751.
[26] A.D. Vaz, S.J. Pernecky, G.M. Raner, M.J. Coon, Peroxo-iron and oxenoid-iron species as alternative oxygenating agents in cytochrome P450-catalyzed reactions: switching by threonine-302 to alanine mutagenesis of cytochrome P450 2B4, Proc. Natl. Acad. Sci. USA 93 (1996) 4644–4648.
[27] T.L. Poulos, Y. Madrona, Oxygen activation and redox partner binding in cytochromes P450, Biotechnol. Appl. Biochem. 60 (2013) 128–133.
[28] T. Imai, H. Globerman, J.M. Gertner, N. Kagawa, M.R. Waterman, Expression and purification of functional human 17α-hydroxylase/17,20-lyase (P450c17) in *Escherichia coli*. Use of this system for study of a novel form of combined 17α-hydroxylase/17,20-lyase deficiency, J. Biol. Chem. 268 (1993) 19681–19689.
[29] B.J. Brock, M.R. Waterman, Biochemical differences between rat and human cytochrome P450c17 support the different steroidogenic needs of these two species, Biochemistry 38 (1999) 1598–1606.
[30] T.A. Pechurskaya, O.P. Lukashevich, A.A. Gilep, S.A. Usanov, Engineering, expression, and purification of "soluble" human cytochrome P45017α and its functional characterization, Biochemistry 73 (2008) 806–811.
[31] I.G. Denisov, S.G. Sligar, Cytochromes P450 in Nanodiscs, Biochim. Biophys. Acta 2011 (1814) 223–229.
[32] M.A. Schuler, I.G. Denisov, S.G. Sligar, Nanodiscs as a new tool to examine lipid–protein interactions, Methods Mol. Biol. 74 (2013) 415–433.
[33] A. Luthra, M. Gregory, Y.V. Grinkova, I.G. Denisov, S.G. Sligar, Nanodiscs in the studies of membrane-bound cytochrome P450 enzymes, Methods Mol. Biol. 987 (2013) 115–127.
[34] I.G. Denisov, Y.V. Grinkova, A.A. Lazarides, S.G. Sligar, Directed self-assembly of monodisperse phospholipid bilayer Nanodiscs with controlled size, J. Am. Chem. Soc. 126 (2004) 3477–3487.
[35] E.S. Shen, F.P. Guengerich, J.R. Olson, Biphasic response for hepatic microsomal enzyme induction by 2,3,7,8-tetrachlorodibenzo-p-dioxin in C57BL/6J and DBA/2J mice, Biochem. Pharmacol. 38 (1989) 4075–4084.
[36] S.B. Mulrooney, L. Waskell, High-level expression in *Escherichia coli* and purification of the membrane-bound form of cytochrome b5, Protein Expr. Purif. 19 (2000) 173–178.
[37] T. Omura, R. Sato, The carbon monoxide-binding pigment of liver microsomes: solubilization, purification, and properties, J. Biol. Chem. 239 (1964) 2379–2385.
[38] Y.V. Grinkova, I.G. Denisov, S.G. Sligar, Functional reconstitution of monomeric CYP3A4 with multiple cytochrome P450 reductase molecules in Nanodiscs, Biochem. Biophys. Res. Commun. 398 (2010) 194–198.
[39] M. Gregory, I.G. Denisov, Y.V. Grinkova, Y. Khatri, S.G. Sligar, Kinetic solvent isotope effect in human P450 CYP17A1 mediated androgen formation: evidence for a reactive peroxoanion intermediate, J. Am. Chem. Soc. 135 (2013) 16245–16247.
[40] H. Shimada, S.G. Sligar, H. Yeom, Y. Ishimura, Heme Monoxygenases – A chemical mechanism for cytochrome P450 oxygen activation, in: T. Funaniki (Ed.), Oxygenases and Model systems, Kluwer Academic Publisher, London, 1997, pp. 195–221.

[41] R.J. Auchus, T.C. Lee, W.L. Miller, Cytochrome b5 augments the 17,20-lyase activity of human P450c17 without direct electron transfer, J. Biol. Chem. 273 (1998) 3158–3165.
[42] C.E. Flück, W.L. Miller, R.J. Auchus, The 17,20-lyase activity of cytochrome P450c17 from human fetal testis favors the Δ5 steroidogenic pathway, J. Clin. Endocrinol. Metab. 88 (2003) 3762–3766.
[43] S. Nakajin, M. Takahashi, M. Shinoda, P.F. Hall, Cytochrome b5 promotes the synthesis of Δ16-C19 steroids by homogeneous cytochrome P-450 C21 side-chain cleavage from pig testis, Biochem. Biophys. Res. Commun. 132 (1985) 708–713.
[44] P. Swart, N. Lombard, A.C. Swart, T. van der Merwe, B.A. Murry, M. Nicol, J. Ian, Mason, Ovine steroid 17α-hydroxylase cytochrome P450: characteristics of the hydroxylase and lyase activities of the adrenal cortex enzyme, Arch. Biochem. Biophys. 409 (2003) 145–152.
[45] M.X. Zuber, E.R. Simpson, M.R. Waterman, Expression of bovine 17α-hydroxylase cytochrome P-450 cDNA in nonsteroidogenic (COS 1) cells, Science 234 (1986) 1258–1261.
[46] K.H. Storbeck, A.C. Swart, J.T. Slabbert, P. Swart, The identification of two CYP17 alleles in the South African angora goat, Drug Metab. Rev. 39 (2007) 467–480.
[47] D.F. Estrada, J.S. Laurence, E.E. Scott, Substrate-modulated cytochrome P450 17A1 and cytochrome b5 interactions revealed by NMR, J. Biol. Chem. 288 (2013) 17008–17018.

JACS
JOURNAL OF THE AMERICAN CHEMICAL SOCIETY
Article
pubs.acs.org/JACS
Terms of Use

Mechanism of the Third Oxidative Step in the Conversion of Androgens to Estrogens by Cytochrome P450 19A1 Steroid Aromatase

Francis K. Yoshimoto and F. Peter Guengerich*

Department of Biochemistry, Vanderbilt University School of Medicine, Nashville, Tennessee 37232-0146, United States

Supporting Information

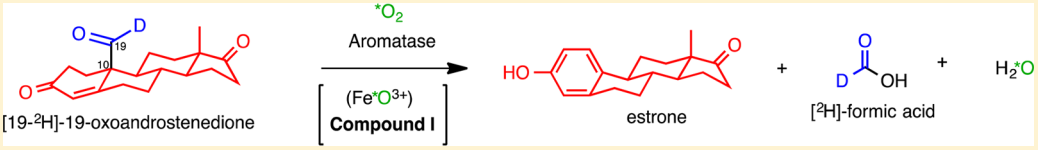

ABSTRACT: Aromatase is the cytochrome P450 enzyme that cleaves the C10−C19 carbon−carbon bond of androgens to form estrogens, in a three-step process. Compound I (FeO^{3+}) and ferric peroxide (FeO_2^-) have both been proposed in the literature as the active iron species in the third step, yielding an estrogen and formic acid. Incubation of purified aromatase with its 19-deutero-19-oxo androgen substrate was performed in the presence of $^{18}O_2$, and the products were derivatized using a novel diazo reagent. Analysis of the products by high-resolution mass spectrometry showed a lack of ^{18}O incorporation in the product formic acid, supporting only the Compound I pathway. Furthermore, a new androgen 19-carboxylic acid product was identified. The rates of nonenzymatic hydration of the 19-oxo androgen and dehydration of the 19,19-*gem*-diol were shown to be catalytically competent. Thus, the evidence supports Compound I and not ferric peroxide as the active iron species in the third step of the steroid aromatase reaction.

INTRODUCTION

Androgens are converted to estrogens by the steroid aromatase, cytochrome P450 (P450 or CYP) 19A1. This reaction is essential in maintenance of hormone balance.[1,2] P450 19A1 is also an important target for drugs used in treating estrogen-dependent cancers.[3] The conversion of an androgen (androstenedione or testosterone) to an estrogen is a three-step process (Scheme 1, **I** to **IV**). The first two steps are relatively straightforward and can both be rationalized in the context of a perferryl "Compound I" (FeO^{3+}) P450 intermediate (**M7**, Scheme 2).

There has been considerable controversy regarding the mechanism of the third step, however, and at least five proposals have been made, including 1β- and 2β-hydroxylation, 4,5-epoxidation, a concerted Compound I mechanism not involving a stable hydroxyl product, and the use of a preceding ferric peroxide form of the enzyme in the catalytic cycle (**M5**, Scheme 2).[4−15] Computational,[7,8] atom-labeling,[9,12,15] spectroscopic,[6,16] biomimetic model,[17,18] synthesis of proposed intermediates,[10,11] and other approaches[19] have been applied, and the most popular view today is that the FeO_2^- (ferric peroxide) form of the enzyme reacts with the 19-aldehyde (CHO) of the androgen in a nucleophilic attack.[12,20] Crystal structures of human P450 19A1 are now available,[21,22] but these do not resolve the catalytic controversy. The most compelling evidence for the FeO_2^- nucleophilic attack mechanism comes from $^{18}O_2$ labeling studies.[9,12,15,20]

From an incubation of purified P450 19A1 with its third substrate, 19-oxo androgen (Scheme 3, **III-o** or **III-g**), in the presence of ^{18}O-labeled molecular oxygen ($^{18}O_2$), an FeO^{3+} (**M7**, Compound I) mechanism (Scheme 3, step 3b) should not lead to the recovery of an ^{18}O atom in the product formic acid (**Vb**), but an FeO_2^- (**M5**) mechanism (Scheme 3, step 3a) will (**Va**). Akhtar et al.[12,15] reported 60% and 90% incorporation of one ^{18}O atom into formic acid, and Caspi et al.[9] reported 70% incorporation, all in studies with human placental microsomes. These results have provided the major evidence for a FeO_2^- mechanism or possibly a mixed mechanism with the FeO_2^- pathway being dominant (Scheme 3, step 3a).

EXPERIMENTAL SECTION

The experimental procedures are provided in detail in the Supporting Information.

RESULTS

Overall Strategy. Several experimental results would clarify the mechanism of the final aromatization step of P450 19A1 (Scheme 3, steps 3a and 3b). The ferric peroxide (Scheme 3, step 3a) mechanism is supported if: (i) one ^{18}O atom is incorporated into the formic acid product (Scheme 3, **Va**) in the incubation of 19-oxo androgen in atmospheric $^{18}O_2$ with P450 19A1 and (ii) the aldehyde (Scheme 3, **III-o**) is required as the substrate for the carbon−carbon bond cleavage step.

Received: August 9, 2014
Published: September 24, 2014

   dx.doi.org/10.1021/ja508185d | J. Am. Chem. Soc. 2014, 136, 15016−15025

Scheme 1. Three-Step Oxidation of Androgens to Estrogens Catalyzed by P450 19A1 (I to IV)[a]

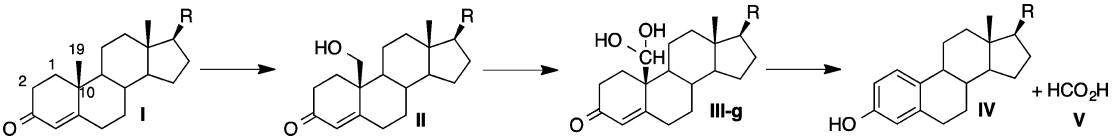

[a]Testosterone → 17β-estradiol, R: −OH; androstenedione → estrone, R: ═O. **III-g**: **III**-*gem*-diol. **III-o**: **III**-oxo.

Scheme 2. Classic P450 Catalytic Cycle[a]

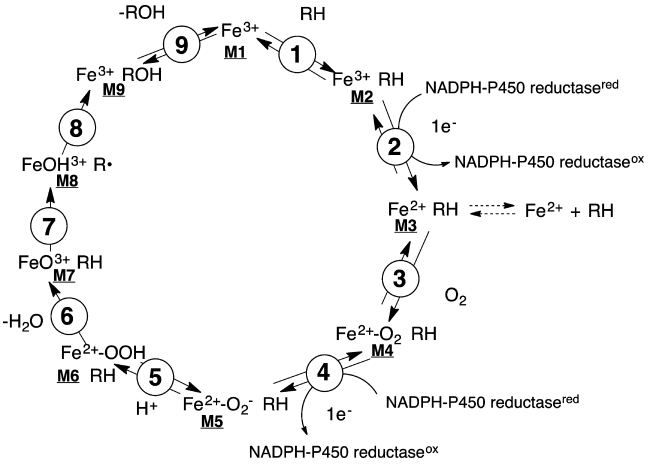

[a]Note the FeO_2^- (**M5**, ferric peroxide) and FeO^{3+} (**M7**, Compound I) forms discussed in the text. Note to reader: in the literature there exists different nomenclature for the same iron intermediates in this P450 catalytic cycle (i.e., **M5**: $Fe^{III}O_2^-$, **M6**: $Fe^{III}O_2H$, **M7**: $(Fe^{IV}O)^{\bullet+}$, **M8**: $Fe^{IV}OH$).[23] For clarity, throughout the text of this manuscript Compound I (**M7**) is referred to interchangeably with FeO^{3+}, and ferric peroxide (**M5**) is referred to interchangeably with FeO_2^-.

In light of the critical nature of the previously reported $^{18}O_2$ incorporation experiments, we re-examined the findings with purified recombinant human P450 19A1 and newer analytical methods. The analysis of trace formic acid is difficult due to the presence of endogenous levels of the compound in laboratory reagents, and (as did Akhtar et al.)[12] we prepared [19-^{2}H]-labeled 19-oxo androstenedione (Figure 2, **4-o**) and testosterone substrates (i.e., 19-CDO androgens) to improve the MS analysis, with a shift of +1 amu (Figure S1, Supporting Information). In addition, a new diazo reagent bearing a pyridine moiety was designed for the mass spectrometric detection of the formic acid enzymatic product using electrospray ionization in the positive mode. However, the analysis is still complicated by the ^{13}C natural abundance contribution (1.109% of ^{12}C) from endogenous formic acid. Accordingly, high-resolution mass spectrometry (HRMS) was used (at a resolution of 100 000) to distinguish $^2HCO_2H$ from the $H^{13}CO_2H$ natural abundance peak present in endogenous formic acid.

Second, the enzymatic and nonenzymatic rates of oxygen exchange between the 19-aldehyde (Scheme 3, **III-o**) and water would indicate whether or not the aldehyde is required as the substrate for the third step. Several case scenarios can arise from the oxygen exchange rate measurements. One is if the nonenzymatic *gem*-diol dehydration rate to the aldehyde (Scheme 3, nonenzymatic $k_{dehydration}$, **III-g** to **III-o**) is faster than the enzymatic rate of 19-hydroxy androgen to estrogen (Scheme 3, **II** to **IV**), then either the aldehyde or the *gem*-diol is a possible substrate for the final step. The method to determine the *gem*-diol dehydration rate ($k_{dehydration}$) requires two experimental measurements: the distribution of the *gem*-diol

Scheme 3. Mechanisms of P450 19A1 Oxidation of Androgens (Rings A and B Shown)[a]

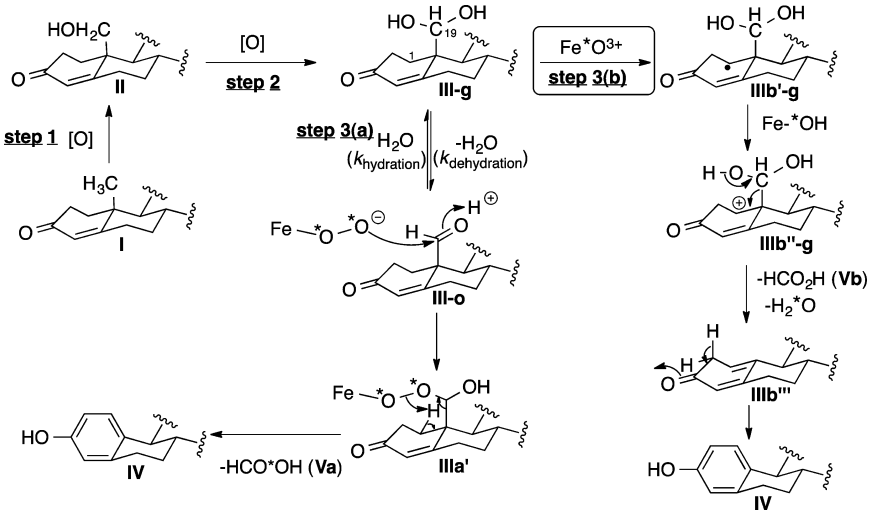

[a]Steps 1 and 2 are generally agreed to involve the P450 FeO^{3+} entity and hydrogen atom abstraction/oxygen rebound.[19] Two possibilities are shown for Step 3 in the presence of $^{18}O_2$. In Step 3a, the FeO_2^- entity participates in a nucleophilic attack on the 19-aldehyde **III-o** (**III-o**: **III-oxo**). In Step 3b, the FeO^{3+} form of the P450 19A1 abstracts the 1β-hydrogen atom of *gem*-diol **III-g** (**III-g**: **III**-*gem*-**diol**). Electron transfer yields the carbocation **IIIb″-g**, which collapses to yield the estrogen product **IV**. In Step 3a, the formic acid must contain label (^{18}O) but not in Step 3b. "*O" = "^{18}O". The step 3(b) pathway is supported by the current study.

Scheme 4. Hydration of the Radical Aldehyde Intermediate (IIIb′-o to IIIb′-g) in the Compound I Mechanism (Step 3b) Pathway

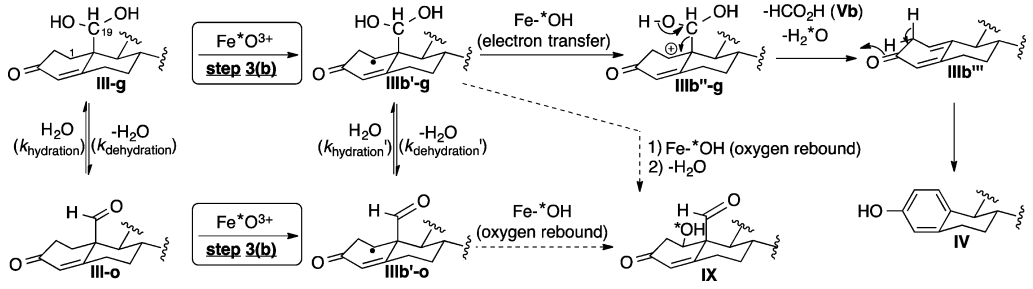

and aldehyde in water through proton NMR (K_{eq}) and the exchange rate of the aldehyde oxygen in water over time (k_{obs}). The latter measurement (k_{obs}) is more challenging in that the synthesis of a 19-[^{18}O]-labeled 19-oxo androgen compound is required. The ^{18}O-labeled 19-oxo androgen was exposed to unlabeled water ($H_2{}^{16}O$) and extracted at time intervals with methyl *tert*-butyl ether (MTBE), followed by subsequent measurement of the ^{18}O-abundance by mass spectrometry. (Our preliminary studies with unlabeled 19-oxoandrostenedione in ^{18}O-labeled water ($H_2{}^{18}O$) resulted in the incorporation of ^{18}O atoms into the 3- and 17-ketone groups, which complicated the measurements for detecting the aldehyde oxygen exchange.)

If the nonenzymatic *gem*-diol to aldehyde dehydration rate is slower than the enzymatic estrogen formation rate from 19-hydroxy androgen (**II** to **IV**), then the comparison to the enzymatic dehydration rate is necessary to show whether or not the enzyme catalyzes the dehydration of the *gem*-diol to the aldehyde. The ferric peroxide mechanism would be supported in the case where the enzyme catalyzes the dehydration of the *gem*-diol (Scheme 3, enzymatic $k_{dehydration}$: **III-g** to **III-o**), while the Compound I mechanism could potentially use either the aldehyde (**III-o**) or the *gem*-diol (**III-g**) as the substrate (water may hydrate the aldehyde to the *gem*-diol at the radical intermediate stage if Compound I initially abstracts the 1β-hydrogen atom of aldehyde **III-o**, Scheme 4: **IIIb′-o** to **IIIb′-g**). In order to simplify our results, we present the data obtained with the androstenedione series in this report; however, the results from the testosterone series are consistent with the androstendione work and are included in the Supporting Information.

New Diazo Reagent for Formic Acid Detection by MS (ESI-Positive Mode). We designed and synthesized a new diazoalkane reagent (1-diazo-3-(3-pyridinyl)propane, **2**) for formic acid derivatization and analysis, in order to utilize liquid chromatography (LC)−mass spectrometry (MS) for increased sensitivity. The diazo reagent (**2**) was accessed by treating a nitrosourea precursor with base. Freshly prepared diazo reagent (**2**) was added directly to an extract of the incubation that was treated with HCl at 0 °C. Control experiments established that significant oxygen exchange of the formic acid (<6%) did not occur with the medium ($H_2{}^{18}O$) under these conditions (Figure 1).

When [19-$^2H_1$]-19-oxo-androstenedione (**4-o**) or -testosterone was incubated with P450 19A1, no label (≤2%, limit of detection) derived from $^{18}O_2$ was recovered in the formic acid product (detected as formate ester **3b**) in three separate experiments with each substrate (Figures S4 and S5, Supporting Information, one data set shown for each). These results are in contrast with those reported previously by Akhtar et al.[12,15] and Caspi et al.[9] The isotopic labeling patterns can clearly be seen in the LC−MS traces (**3b** vs **3c**) and in the full spectra generated in the analyses (Figure 2 and Figures S4 and S5, Supporting Information). In control experiments, P450 3A4 routinely incorporated >98% of the label (one atom) from $^{18}O_2$ in the oxidation of testosterone to 6β-hydroxytestosterone, as expected[24] (this control experiment was done along with each set of incubations with P450 19A1) (Figure S3, Supporting Information).

19-Carboxylic Acid Product Supports Compound I Formation. Our previous work on the kinetics and processivity of androstenedione oxidation by purified P450 19A1 had shown slightly less estrone produced than androstenedione oxidized in single turnover assays,[25] suggestive of additional products. Careful analysis of the oxidation of 19-oxo-androstenedione and -testosterone revealed the presence of two new peaks in each case, either using LC−MS (Figure S6, Supporting Information) or ^{14}C-HPLC (Figure S7, Supporting Information). One product is the 19-CO_2H (19-oic acid) derivative, and this assignment was confirmed by coincident chromatography with an authentic sample in the case of androstenedione 19-oic acid, as well as by MS analysis of the propylpyridine ester derivatives (**6a** and **6b**, Figure 3 and Figure S6 of Supporting Information).

From the knowledge of this novel 19-oic acid aromatase product, a Compound I mechanism suggests a distribution of products arising from a 1β-hydrogen atom abstraction or a 19-hydrogen atom abstraction of the 19-oxo androgen substrate to yield either the estrogen or carboxylic acid, respectively, in the incubation with P450 19A1. Although the 19-oic acid product is minor based on the [4-^{14}C]-androstenedione substrate incubation with P450 19A1 (~95:5, estrogen:carboxylic acid, Figure S8 of Supporting Information), the derivatization of products with the diazo reagent (**2**) allowed for simultaneous detection of the derivatized carboxylic acid and estrogen products in one LC−MS run in the ESI-positive mode. The diazo reagent (**2**) had reacted with the carboxylic acid group of 19-oic androstenedione (**5b**) to afford the ester (**6b**) and also reacted with the phenol moiety of estrone (**4A**) to furnish a phenolic ether (Figure S11, Supporting Information). The use of a deuterium-labeled substrate such as [19-^{2}H]-19-oxoandrostenedione (**4-o**) as the substrate suggests a possible metabolic switching[26] to favor the formation of estrone over 19-oic androstenedione when compared to the use of 19-oxoandrostenedione (nondeuterated, **7b−o**) as the substrate. Indeed, the product partition changed to yield an increased formation of estrogen relative to carboxylic acid when [19-^{2}H]-19-oxoandrostenedione (**4-o**) was used in comparison to 19-oxoandrostenedione (**7b−o**) as the substrate (Figure S11, Supporting Information). This observed metabolic switching

dx.doi.org/10.1021/ja508185d | J. Am. Chem. Soc. 2014, 136, 15016−15025

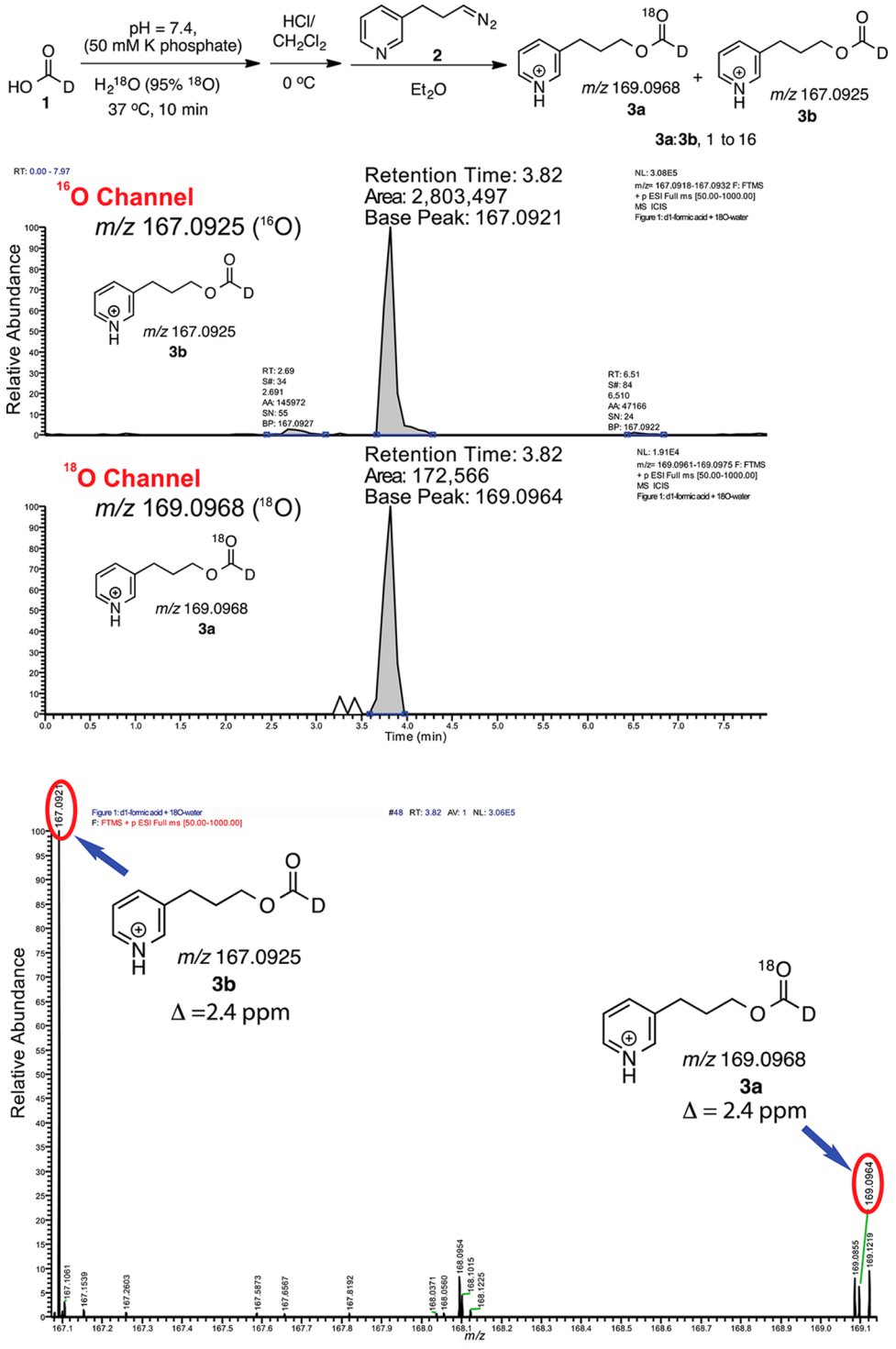

Figure 1. Control experiment confirming minimal exchange between oxygen of [^{2}H]-formic acid (**1**) and medium during the derivatization process (<6% ^{18}O exchange). (A) Ion chromatogram scanning for exact masses with a 4 ppm mass tolerance. (B) Mass spectrum (*m*/*z* 167.0721−169.1413).

supports the Compound I pathway as the active iron species in the reaction of P450 19A1 with its 19-oxo androgen substrate.

In addition, another product (M + 18) was formed from both 19-oxo androgen substrates (from $^{18}O_2$) (Figures S6, Supporting Information), corresponding to the addition of a single oxygen atom, but the site of oxidation has not been established. The 19-oic acid had been reported to be present in hog follicles[27] but had not actually been demonstrated to be an aromatase product. This product (the 19-oic acid of either androstenedione or testosterone) appears to be stable and was not converted to an estrogen (or 19-norandrogen) in P450 19A1 incubations. The identity of the mono-oxygenated aldehyde product is unknown; like the 19-oic acid, it appears to be an end product (Figure S8, Supporting Information). Moreover, the 19-oic androstenedione derivative contained an ^{18}O atom, which confirms the retention of the oxygen atoms in

dx.doi.org/10.1021/ja508185d | J. Am. Chem. Soc. 2014, 136, 15016−15025

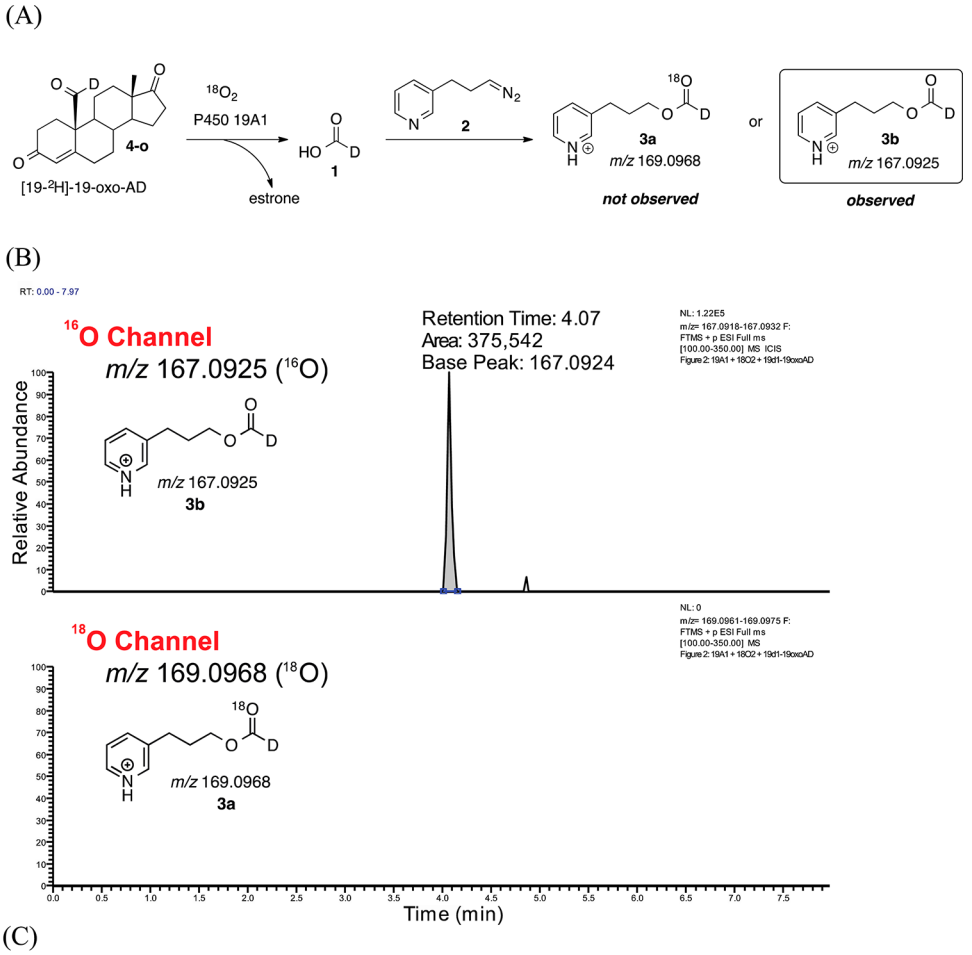

Figure 2. continued

dx.doi.org/10.1021/ja508185d | J. Am. Chem. Soc. 2014, 136, 15016−15025

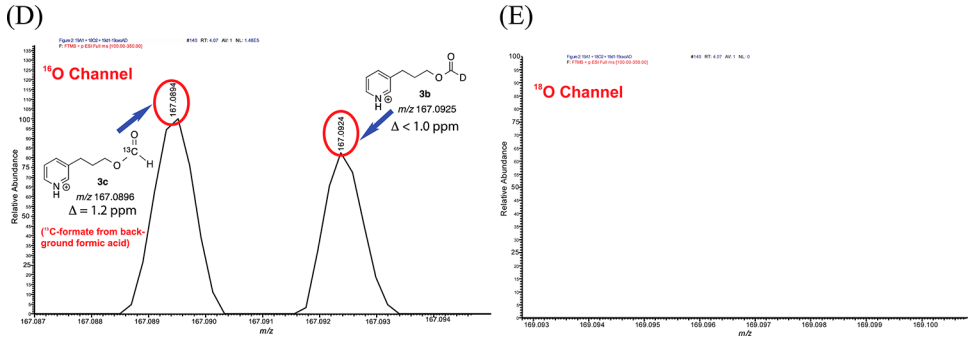

Figure 2. (A) Schematic depicting purified P450 19A1 incubation with [19-^{2}H]-19-oxoandrostenedione **4-o** ([19-^{2}H]-19oxoAD) in the presence of $^{18}O_2$ followed by derivatization with diazo reagent **2**. (B) LC−MS analysis of the deuterated formic acid incubation product, which was derivatized to the formate ester **3b**. The masses of the formates with one ^{18}O atom (**3a**, m/z 169.0968) and no ^{18}O atom (**3b**, m/z 167.0925) were scanned within a window of 4 ppm. No incorporation of the ^{18}O atom was detected. (C) Mass spectrum (m/z 167.0721−169.1413) corresponding to the 4.07 min retention time. An unknown impurity with a mass of m/z 169.1051 was also detected, which is 25 ppm different from the mass of **3a** (m/z 169.0968). (D) Mass spectrum of the formate product (m/z 167.0870−167.0940 range) corresponding to the 4.07 min retention time. Background formate contribution was detected as [^{13}C]-formate ester **3c** (m/z 167.0896). (E) Mass spectrum in the range of the ^{18}O-incorporated formate (m/z 169.0960−169.0980 range) corresponding to the 4.07 min retention time.

carboxylic acid functional groups during the workup conditions of the incubation (cf. Figure 1 control experiment and also with the detection of 19-oic testosterone derivative by LC−MS). Hahn and Fishman had previously identified 2β-hydroxy-19-oxoandrostenedione in incubations with human placental microsomes.[10,11]

19-Aldehyde Oxygen Exchange with Water. One of the differences between the $(FeO)^{3+}$ and FeO_2^- mechanisms is that the former species is an electrophile and the latter a nucleophile (Scheme 3). The nucleophilic FeO_2^- attack mechanism requires an aldehyde and not the *gem*-diol (Scheme 3, step 3a). If a *gem*-diol is the product of the hydroxylation of the 19-carbinol in the second reaction of the sequence (Scheme 1, **III-g**), then a finite time is required for dehydration to form the aldehyde (**III-o**).[28]

19-CH^{18}O-labeled androstenedione (**7a−o**) was synthesized (Figure S2, Supporting Information) to measure the exchange rate with $H_2{}^{(16)}O$ using LC-MS. The strategy involved subjecting the ^{18}O-labeled steroid to unlabeled water followed by extraction and derivatization with $NaBH_4$ at low temperature, to chemoselectively reduce the aldehyde to an alcohol (Figure 4A, **8a** or **8b**). This reduction to 19-hydroxyandrostenedione (**8a** and **8b**) would prevent any further exchange of the 19-oxygen atom with the aqueous mobile phase during LC−MS analysis (Figure 4A).

The observed rate k_{obs} is the sum of $k_{hydration}$ plus $k_{dehydration}$ (i.e., forward and reverse rates),[29] and from measurement of the equilibrium constants (*gem*-diol/aldehyde) by ^{1}H NMR (Figure 4B and Figure S9, Supporting Information) the individual rates can be estimated (Figure S10, Supporting Information). The ratio of the *gem*-diol to the aldehyde (**7b−g** to **7b−o**) was determined to be 1.5:1.0 in D_2O at a pH of 7.8 (adjusted with potassium phosphate) by ^{1}H NMR. The apparent rates of hydration of the aldehyde and dehydration of the *gem*-diol, both $\geq$0.5 s^{-1} for 19-oxoandrostenedione, were greater than k_{cat} for conversion of the androstenedione 19-alcohol to estrone (0.13 s^{-1}, Scheme 1, **II** to **IV**) and therefore are catalytically competent steps.[25] Hence, either the *gem*-diol (**7b−g**) or the aldehyde (**7b−o**) could be a substrate for oxidation by the FeO^{3+} intermediate, and possible mechanisms of oxidations of both to the carboxylic acid have been presented.[4] These results contradict the lack of exchange of the aldehyde oxygen reported by Akhtar et al.,[12] most likely due to insolubility problems resulting from the higher concentration of steroid in water (current report: <10 μM, Akhtar report:[12] 300 μM), which we also noted in our NMR and MS work. Specifically, in regard to the ^{1}H NMR experiments, at higher concentrations of 19-oxoandrostenedione in D_2O (>100 μM or saturated concentration), the 19,19-*gem*-diol proton (8.46 ppm) was not detectable. Moreover, during the time course measurements of the aldehyde oxygen exchange with [19-^{18}O]-19-oxoandrostenedione (**7a−o**) in unlabeled water, the ^{18}O atom remained intact even after 3 h (when the concentration was increased to >100 μM).

DISCUSSION

A scheme consistent with all of the results is shown (Scheme 5), based on a proposal by Covey et al.[30] and modified by Hackett et al.[8] to include a subsequent internal electron transfer (Scheme 5, **3Ab′** to **3Ab″**) to facilitate the final rearrangement. The FeO_2^- intermediate is excluded, based on the formic acid ^{18}O labeling results. The production of the androgen 19-oic acid (**5b**) provides strong evidence that the FeO^{3+} intermediate can form, through an alternate H atom abstraction (C-19) initiating this reaction (Scheme 5, **7b−g** to **5-r**). Although a mechanism involving the (unhydrated) aldehyde cannot be ruled out, a scheme involving the *gem*-diol (**7b−g**) is more straightforward with regard to formic acid formation (Scheme 5). Additionally, the tautomerization step of the 3-keto group to the enol (Scheme 5, **3Ab‴** to **4A**) may occur before the hydrogen abstraction step (Scheme 5, **7b−g** to **3Ab′**) as proposed in the Hackett report on the basis of density functional theory.[8]

Comparison of our differences in results with those of Akhtar et al.[12,15] and Caspi et al.[9] is difficult due to several major improvements in technology. For example, the previous methods to detect formic acid used a diazo toluene reagent to detect formic acid as benzyl formate (i.e., a minimum of 250 ng of benzyl formate was required for its analysis by the reported method).[31] However, in this current study, we designed a new pyridine-containing diazo reagent (**2**) for the sensitive detection of formic acid by mass spectrometry (14 ng of the derivatized formate was readily detected by our method,

dx.doi.org/10.1021/ja508185d | J. Am. Chem. Soc. 2014, 136, 15016−15025

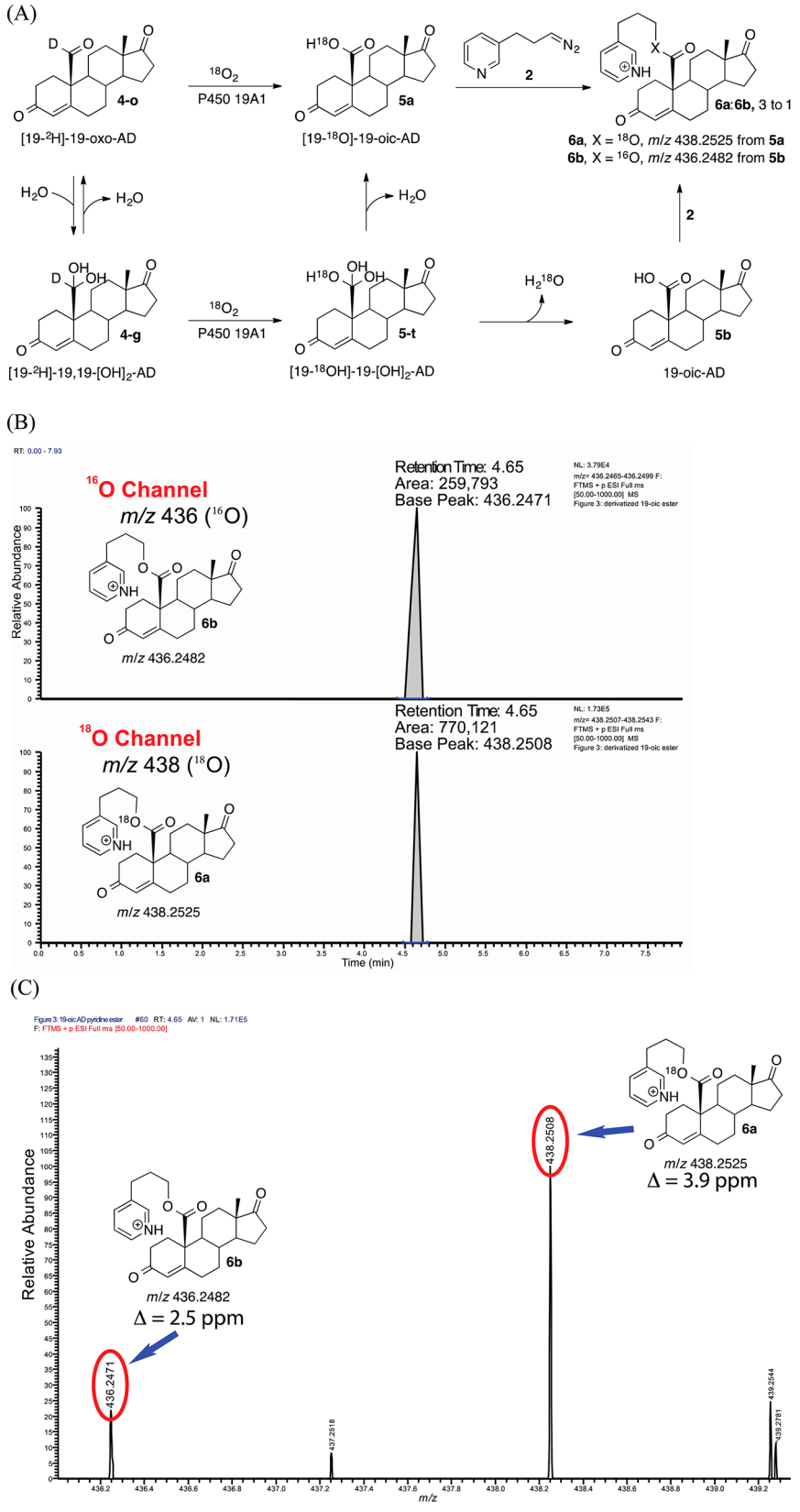

Figure 3. (A) Detection of 19-oic androstenedione as the propylpyridine ester (**6a** or **6b**). (B) High-resolution mass spectrometry trace of the masses scanned with a mass tolerance of 4 ppm for the derivatized carboxylic acid products **6b** and **6a** (m/z 436.2471 and m/z 438.2508) from purified P450 19A1 incubation with [19-^{2}H]-19-oxoandrostenedione ([19-^{2}H]-19oxoAD, **4-o**) in the presence of $^{18}O_2$ followed by derivatization.

Supporting Information) in the positive electrospray ionization mode.

As we have noted previously in this laboratory[32] and known since the earlier aromatase studies,[12] MS analysis of formic acid

dx.doi.org/10.1021/ja508185d | J. Am. Chem. Soc. 2014, 136, 15016−15025

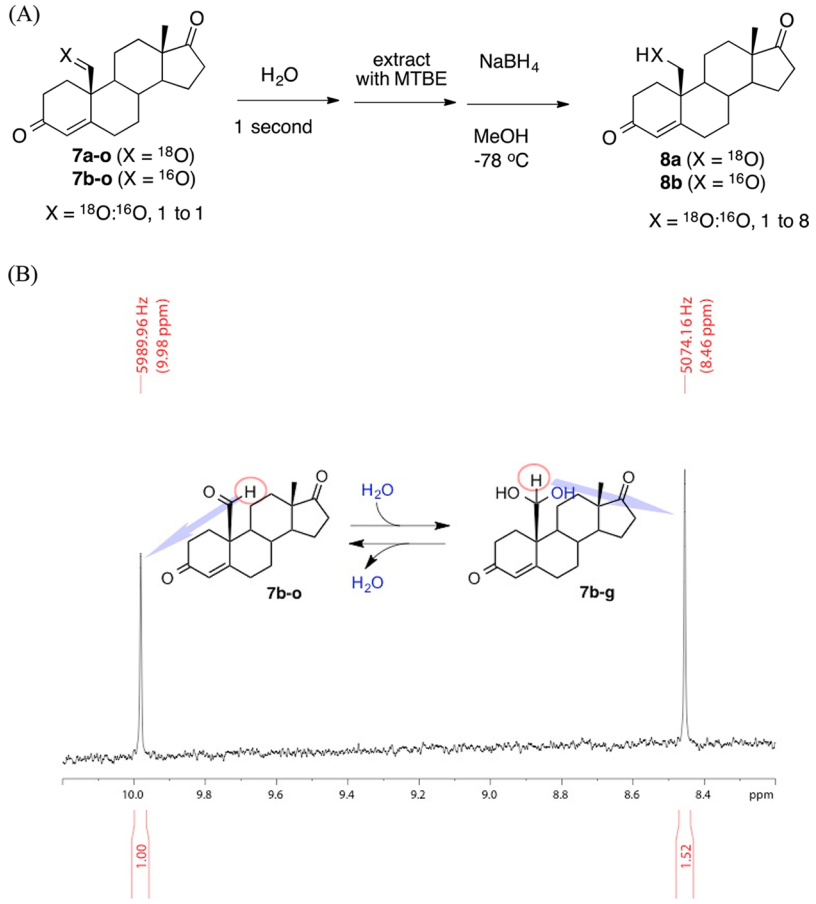

Figure 4. (A) Near complete exchange of the ^{18}O atom after 1 s exposure of [19-^{18}O]-19-oxoandrostenedione to water (50%−11%, ^{18}O abundance from t = 0 s to t = 1 s in water). LC−MS was used to detect isotopic abundance (^{18}O vs ^{16}O). (B) ^{1}H NMR (600 MHz spectrometer) of 19-oxoandrostenedione (**7b−o**) in D_2O (pH 7.8) expanded to show the 10.2−8.2 ppm chemical shift region of the aldehyde (**7b−o**, 9.98 ppm) and *gem*-diol (**7b−g**, 8.46 ppm) C-19 methine protons. MTBE: methyl *tert*-butyl ether.

is not trivial due to the background contamination problem; HRMS clearly reveals the presence of interfering materials (Figure 1 and Figures 2C, S4, and S5, Supporting Information), even with high-resolution LC separation. Prior to use, the laboratory reagents were filtered with basic alumina in order to remove endogenous formic acid; however, the contaminant (**3c**) was still present in the analyses of the incubation products (Figure 2C). In order to completely resolve the [^{2}H]-formate (**3b**, m/z 167.0925) from [^{13}C]-formate (**3c**, m/z 167.0896), a minimum resolution setting of 60 000 on the LTQ Orbitrap mass spectrometer was required (17.4 ppm mass difference between **3b** and **3c**, Supporting Information). The use of low-resolution mass spectrometers such as the one used in the Akhtar report (i.e., AEI MS 30 mass spectrometer with 1000 resolution setting)[31] would definitely not be able to distinguish between the two benzyl formate isotopomers with a 21.9 ppm mass difference (i.e., [^{2}H]-benzyl formate with m/z 137.0582 vs [^{13}C]-benzyl formate with m/z 137.0552). This observation is based solely on our data because there are no mass spectra for the benzyl formates previously published for comparison.[9,12,15] Altogether, our work differs from previous studies in that we used a purified P450 19A1 enzyme, a sensitive new reagent to derivatize formic acid for LC−MS (1-diazo-3-(3-pyridinyl)-propane **2**), and, in particular, HRMS analysis to resolve the formic acid derived from the enzyme incubation (**3b**) and from background contamination (**3c**). Additionally, the use of the new diazo reagent made it possible to detect the novel 19-oic androgen product as the derivatized ester containing an ^{18}O atom (Figure 3, **6a**).

CONCLUSIONS

We conclude that the FeO_2^- mechanism is not operative in the oxidations of either of the 19-oxo androgens to an estrogen and formic acid. Specifically, the supporting evidence includes: (i) the formic acid product did not contain any labeled oxygen atom (^{18}O) from molecular oxygen ($^{18}O_2$), (ii) a 19-oic androgen product was detected, suggesting the utilization of Compound I in the third step, which can abstract either the 1β- or 19-hydrogen atom of the 19-oxo androgen substrate to form either the estrogen or carboxylic acid, respectively, and (iii) the rate of oxygen exchange of the [19-^{18}O]-19-oxoandrostenedione compound in unlabeled water was measured (k_{obs}), and the nonenzymatic rates of $k_{hydration}$ and $k_{dehydration}$ were determined to be catalytically competent and thus support the likelihood that the 19,19-*gem*-diol intermediate can be the substrate for the third step.

The FeO^{3+} mechanism best explains the results, with a semiconcerted reaction without stable intermediates (Scheme 5). These findings are consistent with recently reported results from resonance Raman spectroscopy[6] and kinetic solvent isotope effects[19] from the laboratories of Sligar and Kincaid. The possibilities of 1β- and 2β-hydroxy intermediates that decompose to estrogens[10,11,33] cannot be unambiguously ruled out, in that the formic acid labeling evidence of Caspi et al.[9]

dx.doi.org/10.1021/ja508185d | J. Am. Chem. Soc. 2014, 136, 15016−15025

Scheme 5. Proposed Catalytic Mechanism of the Third Step of Androgen Oxidation by P450 19A1[a]

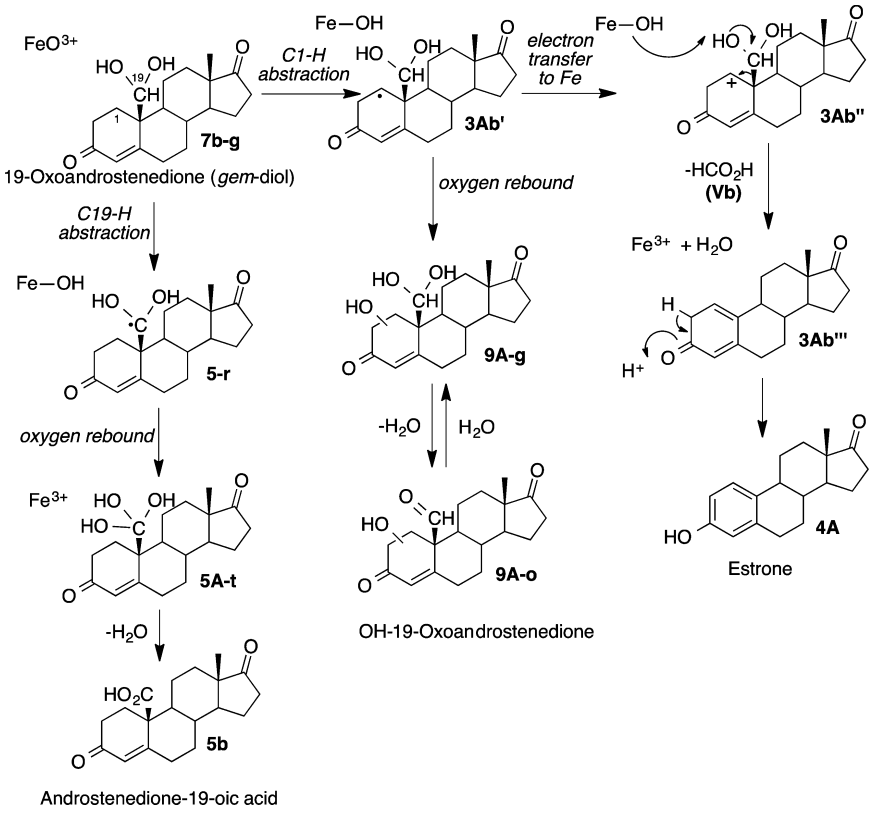

[a]The reaction begins with abstraction of the 1β-hydrogen atom by FeO^{3+}. Further electron transfer, as proposed by Hackett et al.,[8] yields the C-1 carbocation **3Ab″**, and proton abstraction from the *gem*-diol by Fe−OH and rearrangement yields formic acid (**Vb**) and subsequently estrone **4A**. Alternatively oxygen rebound can occur to the A ring to yield the hydroxyl 19-aldehyde (**9A-o**) seen by LC−MS; this may be the product reported to be the 2β-hydroxy 19-aldehyde by Fishman and associates.[10,11] In an alternative initial reaction, FeO^{3+} abstracts the C-19 hydrogen atom. Oxygen rebound yields a *gem*-triol **5A-t**, which degrades to the 19-carboxylic acid, identified here. **5-r**: **5**-radical. **5A-t**: **5A**-triol.

against a role for a 2β-hydroxy intermediate may be suspect in light of the issues with the ^{18}O formic acid analysis. However, the rate of nonenzymatic decomposition of 2β-hydroxy 19-oxoandrostenedione (0.0013 s^{-1} at pH 7.4)[34] is too slow to be catalytically competent (cf. k_{cat} 0.42 s^{-1} for the conversion of the 19-oxoandrostenoedione to estrone)[25] (the rate has not been measured in the presence of enzyme).

Some other P450 enzymes have also been proposed to utilize FeO_2^- chemistry.[20] We do not know if our conclusions with P450 19A1 apply to these, although our approach may be employed. However, the steroid aromatase reaction is best explained by classic FeO^{3+} chemistry (Scheme 5).

■ ASSOCIATED CONTENT

Supporting Information

Experimental methods, syntheses, and figures as described in the text. This material is available free of charge via the Internet at http://pubs.acs.org.

■ AUTHOR INFORMATION

Corresponding Author

f.guengerich@vanderbilt.edu

Notes

The authors declare no competing financial interest.

■ ACKNOWLEDGMENTS

We thank C. D. Sohl for some preliminary studies on rates of oxygen isotope exchange, M. W. Calcutt and B. Hachey for MS assistance and advice regarding formic acid analysis, D. Stec for NMR assistance, L. M. Folkmann and L. D. Nagy for preparation of NADPH-P450 reductase, and K. Trisler for assistance in preparation of the manuscript. This work was supported by National Institutes of Health grants R37 CA090426 and T32 ES007028.

■ REFERENCES

(1) Meyer, A. S. *Biochim. Biophys. Acta* **1955**, *17*, 441−442.
(2) Ryan, K. J. *Biochim. Biophys. Acta* **1958**, *27*, 658−662.
(3) Brodie, A. M. H. *Biochem. Pharmacol.* **1985**, *34*, 3213−3219.
(4) Guengerich, F. P.; Sohl, C. D.; Chowdhury, G. *Arch. Biochem. Biophys.* **2011**, *507*, 126−134.
(5) Cole, P. A.; Robinson, C. H. *J. Med. Chem.* **1990**, *33*, 2933−2944.
(6) Mak, P. J.; Luthra, A.; Sligar, S. G.; Kincaid, J. R. *J. Am. Chem. Soc.* **2014**, *136*, 4825−4828.
(7) Sen, K.; Hackett, J. C. *Biochemistry* **2012**, *51*, 3039−3049.
(8) Hackett, J. C.; Brueggemeier, R. W.; Hadad, C. M. *J. Am. Chem. Soc.* **2005**, *127*, 5224−5237.
(9) Caspi, E.; Wicha, J.; Arunachalam, T.; Nelson, P.; Spiteller, G. *J. Am. Chem. Soc.* **1984**, *106*, 7282−7283.
(10) Hahn, E. F.; Fishman, J. *J. Biol. Chem.* **1984**, *259*, 1689−1694.
(11) Goto, J.; Fishman, J. *Science* **1977**, *195*, 80−81.
(12) Akhtar, M.; Calder, M. R.; Corina, D. L.; Wright, J. N. *Biochem. J.* **1982**, *201*, 569−580.
(13) Fishman, J. *Cancer Res.* **1982**, *42*, 3277s−3280s.

(14) Morand, P.; Williamson, D. G.; Layne, D. S.; Lopa-Krzymien, L.; Salvador, J. *Biochemistry* **1975**, *14*, 635−638.
(15) Akhtar, M.; Corina, D.; Pratt, J.; Smith, T. *J. Chem. Soc., Chem. Commun.* **1976**, 854−856.
(16) Gantt, S. L.; Denisov, I. G.; Grinkova, Y. V.; Sligar, S. G. *Biophys. Res. Commun.* **2009**, *387*, 169−173.
(17) Cole, P. A.; Robinson, C. H. *J. Am. Chem. Soc.* **1988**, *110*, 1284−1285.
(18) Wertz, D. L.; Sisemore, M. F.; Selke, M.; Driscoll, J.; Valentine, J. S. *J. Am. Chem. Soc.* **1998**, *120*, 5331−5332.
(19) Khatri, Y.; Luthra, A.; Duggal, R.; Sligar, S. G. *FEBS Lett.* **2014**, *588*, 3117−3122.
(20) Ortiz de Montellano, P. R.; De Voss, J. J. In *Cytochrome P450: Structure, Mechanism, and Biochemistry*; Ortiz de Montellano, P. R, Ed.; Kluwer Academic/Plenum Publishers: New York, 2005; pp 183−245.
(21) Ghosh, D.; Griswold, J.; Erman, M.; Pangborn, W. *Nature* **2009**, *457*, 219−223.
(22) Lo, J.; Nardo, G. D.; Griswold, J.; Egbuta, C.; Jiang, W.; Gilardi, G.; Ghosh, D. *Biochemistry* **2013**, *52*, 5821−5829.
(23) Krest, C. M.; Onderko, E. L.; Yosca, T. H.; Calixto, J. C.; Karp, R. F.; Livada, J.; Rittle, J.; Green, M. T. *J. Biol. Chem.* **2013**, *288*, 17074−17081.
(24) Krauser, J. A.; Guengerich, F. P. *J. Biol. Chem.* **2005**, *280*, 19496−19506.
(25) Sohl, C. D.; Guengerich, F. P. *J. Biol. Chem.* **2010**, *285*, 17734−17743.
(26) Yoshimoto, F. K.; Zhou, Y.; Peng, H. M.; Stidd, D.; Yoshimoto, J. A.; Sharma, K. K.; Matthew, S.; Auchus, R. J. *Biochemistry* **2012**, *51*, 7064−7077.
(27) Garrett, W. M.; Hoover, D. J.; Shackleton, C. H.; Anderson, L. D. *Endocrinology* **1991**, *129*, 2941−2950.
(28) Greenzaid, P.; Luz, Z.; Samuel, D. *J. Am. Chem. Soc.* **1967**, *89*, 756−759.
(29) Johnson, K. A. In *Kinetic Analysis of Macromolecules*; Johnson, K. A., Ed.; Oxford University Press: Oxford, UK, 2003; pp 1−18.
(30) Covey, D. F.; Carrell, H. L.; Beusen, D. D. *Steroids* **1987**, *50*, 363−374.
(31) Corina, D. L. *Anal. Biochem.* **1977**, *80*, 639−642.
(32) Chowdhury, G.; Calcutt, M. W.; Guengerich, F. P. *J. Biol. Chem.* **2010**, *285*, 8031−8044.
(33) Osawa, Y.; Yoshida, N.; Fronckowiak, M.; Kitawaki, J. *Steroids* **1987**, *50*, 11−28.
(34) Hosoda, H.; Fishman, J. *J. Am. Chem. Soc.* **1974**, *96*, 7325−7329.